# Control of the Properties of Carbon Fiber-Reinforced Plastics

R.G. White* and T.A. Palmer†
*University of Southampton, Southampton, England*

**This paper describes methods for measuring and controlling the elastic and loss properties of composite materials in the form of carbon fiber-reinforced plastics. The influences of fiber length and matrix properties are examined and it is shown how a compromise between high stiffness-to-weight ratio and internal damping may be sought. Experimental data may be used in anisotropic theory for predicting the free-vibration characteristics of plates; the case of a panel with static in-plane compression is investigated. General comments are made concerning the applicability of simple "engineering" procedures for predicting the dynamic strain response of panel-type structures to random acoustic loading, and the effects of nonlinear behavior are discussed.**

## Nomenclature

$E_c$ = beam flexural modulus
$E_{c_{exp}}$ = experimental value of $E_c$
$E_{c_{theor}}$ = theoretical value of $E_c$
$E_{sp}$ = specific modulus, $= E/\text{specific gravity}$
$D_m$ = material unit damping energy, $= J\gamma_0^n$
$G_R$ = shear modulus of rod
$\beta_R$ = shear loss factor of rod
$\gamma_0$ = shear strain
$\gamma_{0L}$ = shear strain sensitivity limit
$\eta$ = material flexural loss factor
$\eta_c$ = beam flexural damping
$\eta_{exp}$ = experimental value of $\eta$
$\eta_{theor}$ = theoretical value of $\eta$

## I. Introduction

In recent years, the need for stiff lightweight materials in the aeronautical industry has stimulated considerable research into the dynamic properties of carbon fiber-reinforced plastic (CFRP).

Previous studies have revealed that CFRPs, while having a high stiffness-to-weight ratio compared to conventional materials, have low internal damping at fiber volume fractions suitable for high-performance structures. Where acoustic loads are imposed on such structures, fatigue life is a critical parameter. Consequently, it is not only beneficial, but imperative, that resonant responses be limited; i.e., there should be substantial damping.

A program of work has been underway for several years at the Institute of Sound and Vibration Research (ISVR), with the objective of developing a CFRP material or a composite structural configuration compromising between stiffness and damping characteristics by achieving intermediate stiffness and damping properties compatible with high-performance structural requirements.

Two possible methods of improving the dynamic properties of CFRPs are being investigated, viz.: 1) the use of aligned discontinuous fiber reinforcement, perhaps in conjunction with continuous fibers, thus offering greater variability and control of resultant modulus, damping and moldability; and 2) the selection of a highly damped matrix material.

These studies have necessitated the development of both accurate experimental methods and novel molding techniques for the manufacture of specimens. For convenience, material properties have been found via simple experiments on beams and rods but, ultimately, and more relevantly, laminated plate-type structures will be tested. Extensive experimental investigations into the dynamic behavior of structures under the combined action of static, in-plane compression and random acoustic excitation at grazing incidence have been carried out. Results from these experiments were compared with those predicted by an extension of anisotropic plate theory, with substitution of appropriate material constants for each layer.

## II. Specimen Manufacture

In order to carry out a meaningful investigation of the dynamic properties of CFRPs, it is essential that composites may be specified in terms of their constituent materials, i.e., fiber type and length, matrix, fiber volume fraction ($V_f$), and fiber distribution. Having selected the fiber-matrix system, the fiber volume fraction, orientation, and distribution are controlled by the method of molding. Molding techniques used previously at the ISVR[1] were considered to give inadequate control of these parameters when using short aligned fibers. Improved techniques were therefore required for the manufacture of beams, rods, and plates, reinforced with short aligned or random fibers to a specified volume fraction and even fiber distribution.

### A. Manufacture of Beam Specimens

Using the release agent treated mold and layup illustrated in Fig. 1, CFRP beams of aligned short/continuous or random fibers of specified volume fraction and even distribution were produced.

The plunger of the mold had 10 holes of 1.2 mm diameter along each edge, allowing a 20-mm-wide beam to be obtained from the central unmarked portion. Any excess resin in the preimpregnated fiber layers (prepreg) was forced out through these bleed holes during molding. No fibers were forced up the sides of the mold, so the fiber volume fraction could be calculated from the number and fiber content of the prepreg sheets. Stops controlling the resultant thickness of the beam were fitted along the two sides of the mold. The complete mold was then subjected to the temperature and pressure schedule required to cure the resin.

With this molding technique it is possible to mold beams of $V_f$ up to 70% with acceptable uniformity, distribution, and alignment of short fibers.

Presented as Paper 83-0859 at the AIAA/ASME/ASCE/AHS 24th Structures, Structural Dynamics and Materials Conference, Lake Tahoe, Nev., May 2-4, 1983; received May 18, 1983; revision submitted Oct. 26, 1983. 

*Professor and Director, Institute of Sound and Vibration Research.

†Research Assistant, Institute of Sound and Vibration Research.

### B. Manufacture of Rod Specimens

*1. Using Aligned Continuous Fibers*

Fiber tows were laid in a release agent treated mold manufactured of stainless steel and surface ground to a fine tolerance. Both the plunger and body had semicylindrical shapes, so as to produce a rod of 7 mm diameter and 400 mm length. The end plates were reinforced with Tygaflor 103C/stainless steel mesh/Tygaflor 103C forming bleed plates.[2]

*2. Using Aligned Short Fibers*

Prepreg sheets were cut to size and used in the number required for the resultant composite $V_f$. The sheets were then rolled in turn to form a rod of the required length and placed in the mold. The procedure was then as for continuous CFRP (CCFRP) rods noted previously.

### C. Manufacture of Plate Specimens

There are two common methods of molding flat plates; namely, autoclaving and molding in a press. Although the former is more versatile and generally chosen for industrial production, the latter yields more accurate control over plate thickness, a crucial parameter in this study. For this reason, and due to financial and time considerations, press molding was selected as the manufacturing process.

The molding process is then very simple, prepreg sheets being stacked to form a plate such that the fibers in each layer lay in the required direction. After a suitable dwell time the stack was consolidated into a laminate under heat and pressure, according to the resin curing schedule.

Volume fractions and fiber alignments were checked using the acid digestion technique and microscopic studies, respectively.[2]

## III. Dynamic Testing Techniques and Deduction of Specimen Properties

### A. Flexural Tests

The dynamic flexural moduli and loss factors of continuous and short-aligned or random CFRP (CCFRP, SCFRP, and RCFRP, respectively) were estimated using a technique[1,3] which involves the vibration of a free-free beam in its fundamental flexural mode using a noncontacting exciter and response measurement transducer.

The beams were driven at the first resonance frequency. The equivalent flexural moduli $E_c$ were then calculated from the natural frequency equation of a homogeneous Euler beam.

$$E_c = 48\pi^2 f^2 L^3 M / a_n^2 b d^3$$

where $f$ is the first resonance frequency, $L$ the length of the beam, $b$ the width of the beam, $d$ the thickness of the beam, $M$ the mass of the beam, and $a_n$ a constant (22.37 for the first flexural mode).

The beam loss factors were derived from free-vibration waveforms using the logarithmic decrement method.

### B. Torsional Tests

Figure 2 shows the principle and block diagram of the apparatus used to measure the shear loss factors and shear moduli of clamped-clamped rod specimens at a given surface shear strain amplitude under steady-state torsional vibration.

The dynamic torsional load was applied to the two rectangular coils in magnet systems driving a bar attached to the rod at midspan. Since the mass of the test rod could be ignored with respect to the drive assembly, the complete system could be considered as a single-degree-of-freedom system with lumped parameters.

The surface shear strain amplitude of the rod, as indicated by strain gages, was maintained constant as the frequency was varied around resonance by adjustment of the a.c. current

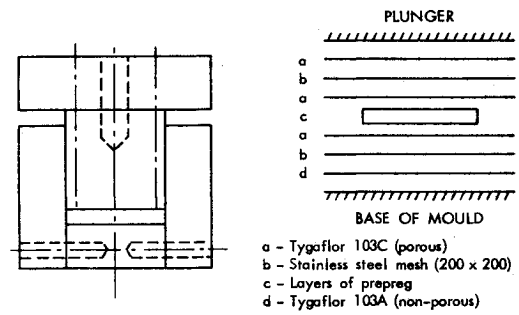


**Fig. 1 Mold and layup used in manufacture of beam specimens.**

**Fig. 2 Block diagram of the equipment used for torsional testing.**

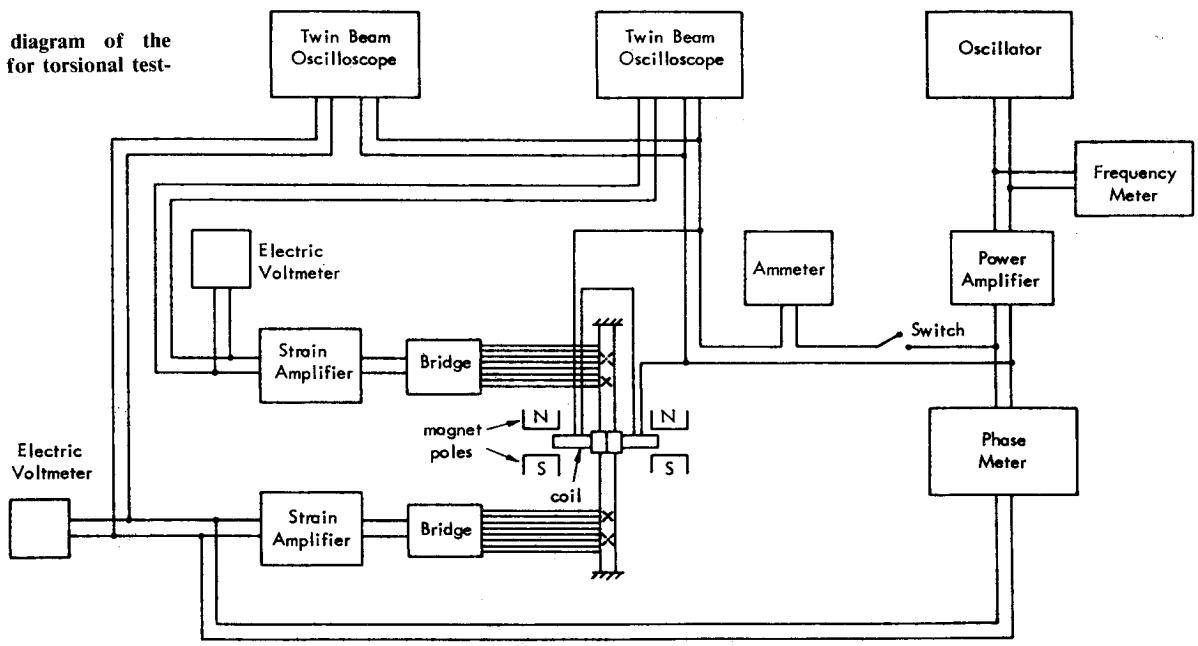

input to the coils. The frequency at minimum input current for a particular shear strain indicated the resonance frequency, from which the shear moduli of the rods were calculated using the natural frequency equation of the system.

$$G_R = (2\pi f_r^2 / R^4) JL$$

where $G_R$ is the shear modulus of the rod, $f_r$ the resonance frequency, $L$ the length of the rod of radius $R$, and $J$ the moment of inertia of the driving system, calculated experimentally as discussed in Ref. 2.

The shear loss factors of the rods $\beta_R$ were measured using two methods carried out simultaneously. The input current to the coils and the phase angle between excitation and response were monitored as the frequency varied around resonance at constant surface shear strain amplitude. By plotting the variation of input current (proportional to force) with frequency around resonance, $\beta_R$ could be derived using the half-power bandwidth.

The second method of estimating $\beta_R$ involved plotting the frequency vs phase, characteristic around resonance at constant response amplitude. The slope of the phase angle against frequency curve at resonance $(d\phi/df)_R$ was measured and estimates of shear loss factor derived according to

$$B_R = 2 \Big/ \left[ f_r \left( \frac{d\phi}{df} \right)_R \right]$$

### C. Combined Loading

An apparatus for measuring stiffness and damping properties of rods under combined dynamic torsion and bending with pretwist and/or pretension is currently being commissioned at the ISVR. The principle of the apparatus is illustrated in Fig. 3.

The rod specimens, when secured into the top and bottom clamps, can be subjected to static tension by removal of a shim between the clamps and the rig body and/or static torsion by securing the bottom clamp and twisting the top clamp through the desired angle.

Oscillatory torque and bending forces then can be applied to the central inertia bar via the two driving coil-magnet units. Suitable choice of polarity and phase shift between the currents in each coil allows excitation in torsion, bending, or combined modes. Two identical magnet-coil units used as voltage generators monitor the system response.

Having adjusted the clamps and input currents as required, the system should be carefully tuned to resonance. Readings of coil displacement (via strain gages) drive coil currents, pick up coil voltages, and supply frequencies enable the energy input to and energy stored in the system to be calculated as detailed in Ref. 4, when

$$B_R = \frac{\text{energy dissipated}}{2\pi \text{ energy stored}}$$

which under steady-state resonance conditions,

$$B_R = \frac{\text{energy supplied}}{2\pi \text{ system kinetic energy}}$$

## IV. Analysis of Results

The following discussion refers to CFRP specimens comprising HM-S fibers and DX210 resin. (See Table 1.)

### A. Flexural Results

The dynamic flexural moduli of elasticity $E_c$ and structural loss factors $\eta_c$ of CCFRP, SCFRP, and RCFRP with various fiber aspect ratios and volume fractions were measured experimentally in flexure using the technique described in the previous section.

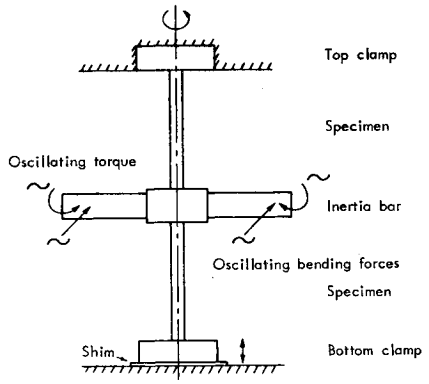


**Fig. 3 Combined loading apparatus**

**Table 1 Properties of high modulus carbon fibers (HM-S) and DX210 resin**

| | |
|---|---|
| HMAS fibers | |
| Young's modulus | 345 GN/m$^2$ |
| Ultimate tensile strength | 2 GN/m$^2$ |
| Specific gravity | 1.87 g/cm$^3$ |
| DX210 resin | |
| Curing agent | 3 parts Epiture $BF_3$-400 per 100 parts resin solid |
| Curing schedule | 4 h at 170°C |
| Flexural strength | 93.8 MN/m$^2$ |
| Flexural modulus | 2.78 GN/m$^2$ |
| Tensile strength | 53.2 MN/m$^2$ |
| Elongation | 3% |
| Specific gravity | 1.21 |

Since the damping of CFRP composites is essentially independent of stress for small-amplitude dynamic behavior, the measured beam loss factors were taken as the material loss factors (i.e., $\eta_c = \eta$) and were compared directly with theoretical estimates.

The moduli of elasticity of CCFRPs were derived theoretically using the law of mixtures, while those of SCFRP and RCFRP necessitated the use of the more complex Cox model[5] or McLean equation.[6] The material loss factors of CCFRPs, SCFRP, and RCFRP were calculated using the ratio of the loss to storage moduli $E_c''/E_c'$ of the complex relationship for $E_c$. In addition, the McLean equation was used to estimate the loss factors of SCFRPs.

Theoretical and experimental results are presented and compared in Figs. 4-7.

From consideration of the experimental and theoretical estimates of $E_c$ and $\eta$ for SCFRPs and RCFRPs, the following observations were drawn:

1) $\eta$ decreased as fiber aspect ratio increased for all volume fractions, the rate with which it varied decreasing with increasing aspect ratio.

2) $\eta$ decreased with increasing $V_f$ for all aspect ratios until $V_f = 65\%$. Above this volume fraction $\eta$ increased with increasing $V_f$ due to interaction between fibers.

3) $E_c$ increased with increasing aspect ratio for all volume fractions, the rate of variation decreasing at high aspect ratios $(\ell/d > 142)$.

4) $E_c$ increased with fiber volume fraction for all aspect ratios.

Comparing theoretical and experimental results, it was found that $E_{c\text{exp}}/E_{c\text{theor}} < 1$ but increased with increasing fiber length for all aspect ratios and volume fractions. This may

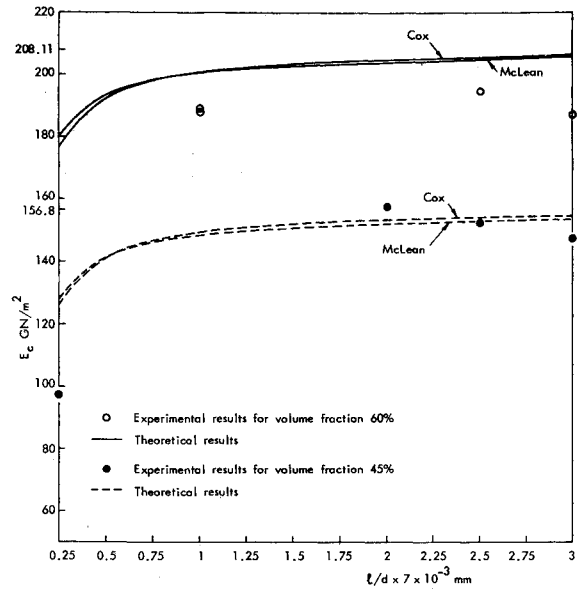


**Fig. 4 Effect of aspect ratio ($l/d$) on $E_c$ of aligned CFRP (HM-S/DX210) composites.**

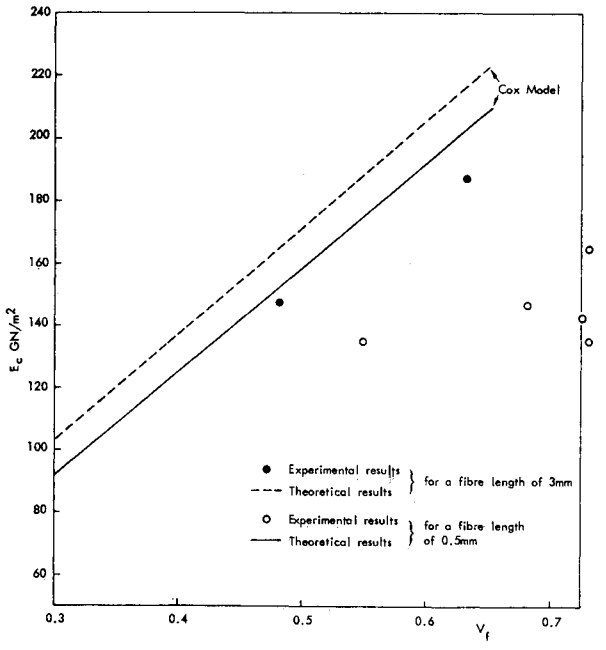


**Fig. 6 The effect of $V_f$ on $E_c$ of aligned short CFRP (HM-S/DX210) composites.**

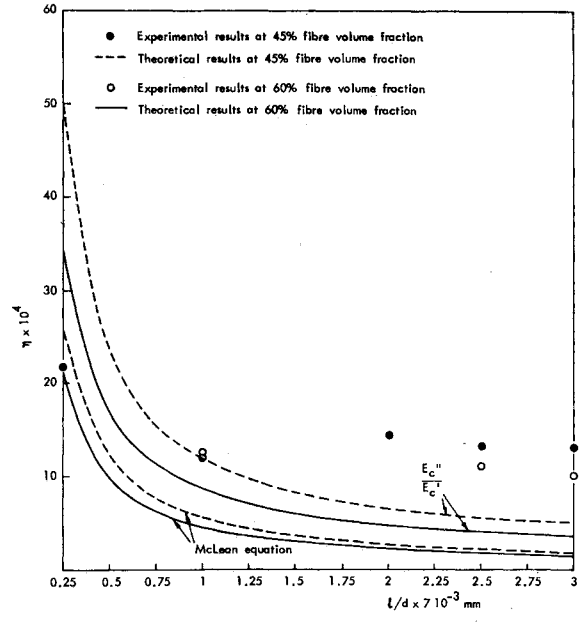


**Fig. 5 Effect of aspect ratio ($l/d$) on $\eta$ of aligned short CFRP (HM-S/DX210) composites.**

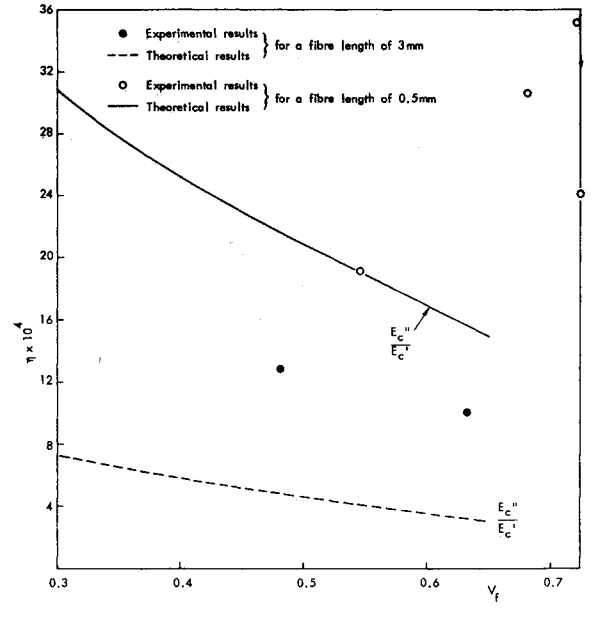


**Fig. 7 The effect of $V_f$ on $\eta$ of aligned short CFRP (HM-S/DX210) composites.**

have been due to: 1) misalignment of the fibers in the beams; 2) experimental values being estimated from dynamic flexural test data whereas theoretical results were calculated from tension data ($E_{\text{tension}} > E_{\text{compression}}$ for CFRPs); 3) interaction between fibers in SCFRPs; 4) load transfer at the ends of fibers which was neglected in the theory; and 5) effect of transverse shear deformation ignored in the theory.

Furthermore, $\eta_{\text{exp}}$ was found to be higher than $\eta_{\text{theor}}$ for all fiber aspect ratios and volume fractions, except for fiber lengths of 0.25 and 0.5 mm at $V_f = 55\%$. This may be a result of: 1) misalignment of the fibers in the beams; 2) aerodynamic damping; 3) damping of CFRP being slightly stress dependent even at small amplitudes; 4) additional damping mechanisms, e.g., interaction between fibers; and 5) effect of transverse shear deformation.

### B. Torsional Results

The dynamic shear moduli $G_R$ and structural shear loss factors $\beta_R$ of a CCFRP rod and SCFRP rods of various fiber lengths at one volume fraction were measured experimentally at various surface shear strain amplitudes using techniques described in Sec. III.

The derivation of material damping from specimen damping is essential if it is intended to fully define the dynamic properties of new materials such as CFRP. Consequently, the experimentally determined shear loss factors derived from the rod specimens were reduced to material loss factor equivalents using methods discussed in Ref. 2. Studies of the material loss factor at various stresses facilitated determination of the unit damping energy $D$, damping constant $J$, and exponent $n$ in the equation

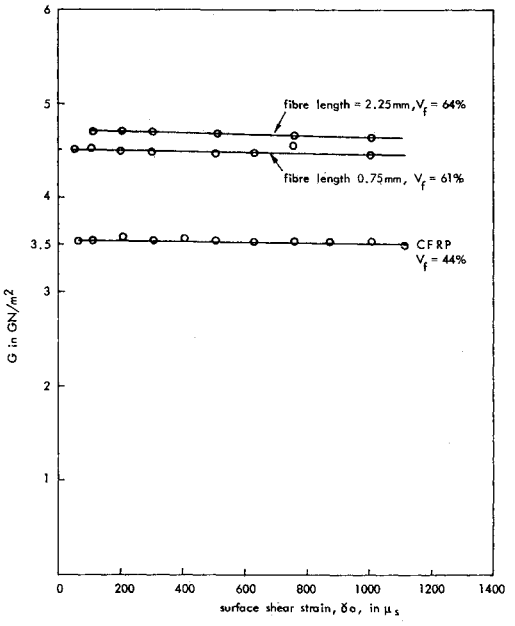


**Fig. 8 The effect of surface shear strain $\gamma_0$ on the shear modulus $G$ of aligned CFRP (HM-S/DX210) composites.**

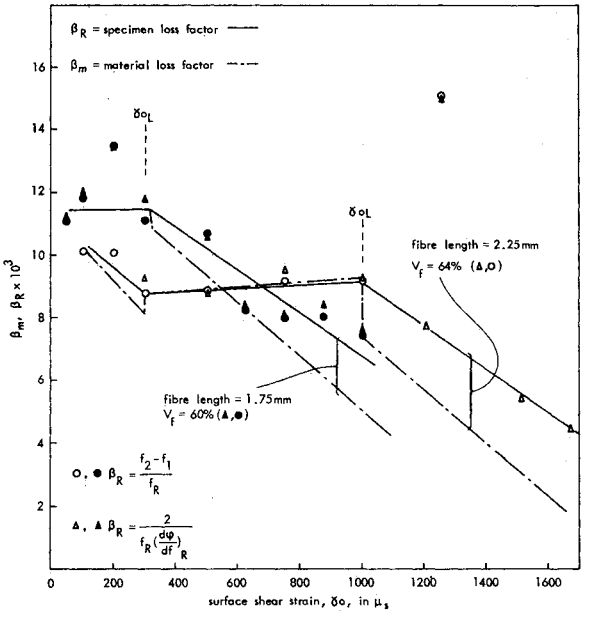


**Fig. 9 The effect of surface shear strain $\gamma_0$ on the structural and material shear loss factors $\beta_R$ and $\beta_m$, respectively, of aligned short CFRP (HM-S/DX210) composites.**

$$D = J\gamma^n$$

A summary of results is given in Figs. 8-11.

Consideration of the experimental estimates of $G_R$ and $\beta_R$ for SCFRP rods indicates that $G_R$ increased, while $\beta_R$ decreased with increasing fiber length. Furthermore, $G_R$ decreased slightly with increasing surface shear strain $\gamma_0$ for all CFRP rods, as was the case for a resin and an aluminum rod.

The structural shear loss factors $\beta_R$ of all the CFRP rod specimens exhibited the same trends in behavior with increasing $\gamma_0$. $\beta_R$ was essentially constant with increasing $\gamma_0$ up to a shear strain sensitivity limit $\gamma_{0L}$, which depended on the fiber length, $V_f$, and degree of alignment. Within the shear strain sensitivity limit, the material loss factor $\beta_m$ was approximately equal to $\beta_R$, i.e., the material exhibited linear damping corresponding to the damping exponent $n = 2$.

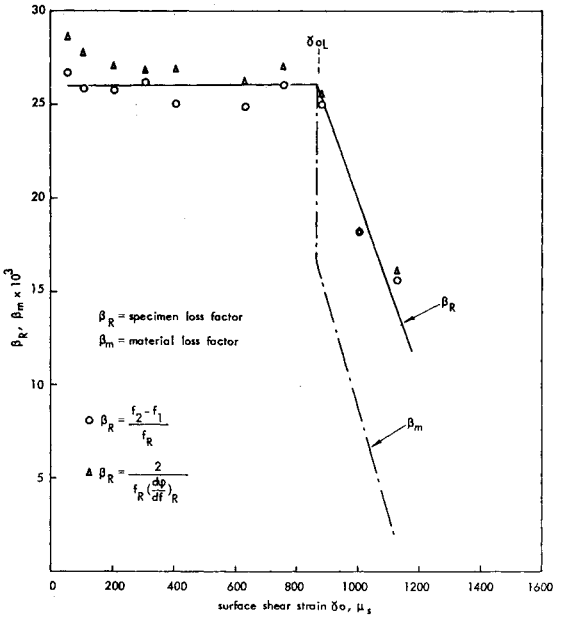


**Fig. 10 The effect of surface shear strain $\gamma_0$ on the structural and material shear loss factors $\beta_R$ and $\beta_m$, respectively, of the unidirectional CFRP (HM-S/DX210) rod of 44% fiber volume fraction.**

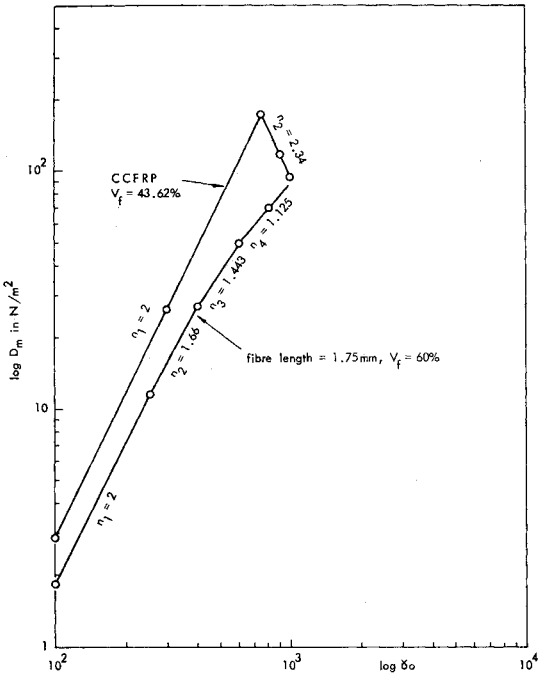


**Fig. 11 The variation of the unit damping energy $D_m$ with maximum shear strain $\gamma_0$ for aligned CFRP (HM-S/DX210) composites.**

At values of $\gamma_0$ greater than $\gamma_{0L}$, $\beta_R$ decreased with increasing $\gamma_0$ in all cases, the rate of decrease depending on the variation of the unit damping energy $D_m$ with $\gamma_0$, there being a dependence on $n$.

$\beta_m$ also increased with increasing $\gamma_0$, but was less than $\beta_R$ in all cases, indicating $n$ to be less than 2, the material damping being nonlinear.

The ratio $\beta_R/\beta_m$ increased with $\gamma_0$ for all of the composite and resin specimens as a result of $n$ decreasing with increasing $\gamma_0$.

It can be concluded therefore that $n$ was a function of shear strain, such that

$$D_m = J(\gamma_0)\gamma_0^{\eta(\gamma_0)}$$

The unit damping energy $D_m$ of a SCFRP increased with increasing fiber length at a given shear strain. This was a result of the maximum shear strain energy increasing with fiber length (due to $G$ increasing at a given shear strain, energy dissipation being a function of strain energy in the material). However, the material loss factor decreased with increasing fiber length as the increase of strain energy in the material was greater than the increase of unit damping energy.

It can be seen that the shear loss factor of a composite material of given $V_f$ is higher than the flexural loss factor. This may be due to higher distortional energy being introduced in the matrix and the higher potential for interfacial slip or high stress concentrations in the matrix (particularly at the interface) in the torsional case.

Therefore, it has been shown that correct choice of fiber aspect ratio and volume fraction may yield SCRFP materials, with improved damping compared to CCFRP, while retaining a high modulus of elasticity.

Investigations are now being carried out into the effect of resin flexibility and damping on resultant composite properties. Using the flexural test procedures of Sec. III, the dynamic flexural stiffness and damping properties of a series of epoxy resin beams were found. Both stiffness and damping varied considerably between resins.

Since the stiffness properties of CFRPs are predominantly derived from the fibers, it would appear that use of a low stiffness resin would not have an appreciably adverse effect on the stiffness of the composite and thus could be tolerated if beneficial to composite damping. This statement was vindicated by carrying out free-free flexural tests on a series of CCFRP beams of constant volume fraction, but with a matrix material having different properties. Results are tabulated in Table 2.

It can be seen that the specific modulus $E_{sp}$ of specimen 9, comprising a resin of $E_{sp} = 3.275$ GNm$^{-2}$ was only 5% greater than that of specimen 8 manufactured of a resin of $E_{sp} = 0.172$ GNm$^{-2}$. However, the loss factor of specimen 8 ($\eta = 0.01$) was 20 times that of specimen 9. Such an internal loss factor is very much greater than that of conventional structural materials under similar loading conditions and, therefore, is to be commended. Unfortunately, the stiffness of the composite in directions other than that of the fiber reinforcement is governed by matrix properties. Consequently, specimen 8 was very weak in torsion and could not be used in structural situations subjected to loads in more than one direction.

However, it is possible to appreciably increase the shear stiffness of a composite by laying up the fibers in the directions of the principal axes. The optimum layup, with respect to stiffness, for a specimen to be subjected to combined tension, torsion, and bending would be $(90, +45, -45, 0)_s$. The consequences of such a layup on loss factors would be to increase the flexural loss factor while decreasing the shear loss factor compared to a unidirectionally aligned specimen.

Alternatively, a high damping resin may be used in conjunction with a stiffer resin and continuous/aligned discontinuous fibers to form a structural configuration as shown in Fig. 12.

It is possible that material properties providing a practical compromise between stiffness and damping under typical loading situations may be attained by one or both of the above methods.

## V. The Free-Vibration Characteristics of Panel-Type Structures

The preceding sections have been concerned with methods for controlling, determining, and predicting the material properties of composites in flexure and shear. Such information is needed if theoretical predictions are to be made for natural frequencies and mode shapes of structures. As has already been discussed above, structures are generally subjected to combined loading in service in the form of a static load with a dynamic load superimposed. In the case of panels or thin stiffened plate-type structures, a static in-plane stress often will be present with superimposed flexural vibration caused by dynamic loading.

The effects of static in-plane compression on panel dynamics have been examined in Refs. 7 and 8. The Rayleigh-Ritz method has been used in a general anisotropic plate theory for the determination of natural frequencies, mode shapes, and critical buckling loads. It is well known that imperfections can be present in composite structures and damage can also occur. To include practical damage in a theoretical model is difficult at present and the latter part of the theoretical work in Ref. 8 included an initial study of damage in the form of an edge crack in a composite plate. A range of plates was examined theoretically and complementary experiments were carried out to measure resonance frequencies and nodal patterns. Good agreement was found between theoretical and experimental natural frequencies, even at high levels of static, in-plane stress approaching buckling. An example of an investigation of crack length effects is given in Fig. 13 for a 16-layer carbon fiber-reinforced plastic plate. The effect of in-plane stress, $\sigma_x$, is clear in the diagram, as is the influence of crack length ratio. This work is currently being extended into the postbuckle regime and, in this study, boundary conditions which are more representative of those met in practical aircraft structures will be used. The panel edges will not be fully fixed, as

**Table 2 Resin and CCFRP beam flexural properties**

| Specimen No. | $E_{sp}$, 1st mode, GN/m$^2$ | $\eta$, 1st mode |
|---|---|---|
| Resin | | |
| 1 | 0.099 | 1.15 |
| 2 | 2.936 | 0.04 |
| 3 | 1.669 | 0.10 |
| 4 | 0.16 | 1.14 |
| 5 | 3.275 | 0.007 |
| 6 | 0.172 | 1.15 |
| 7 | 7.369 | 0.02 |
| CCFRPs (60% $V_f$) | | |
| 8 (Resin 6) | 115.10 | 0.01 |
| 9 (Resin 5) | 121.48 | 0.0005 |
| 10 (Resin 1) | 91.37 | 0.008 |

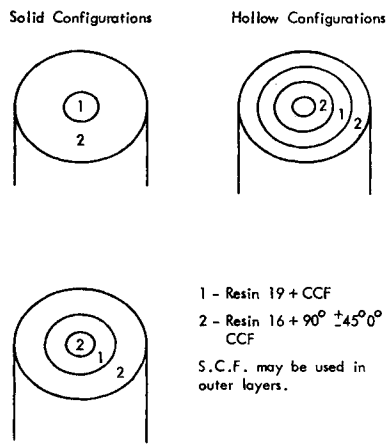


**Fig. 12 Possible structural configurations.**

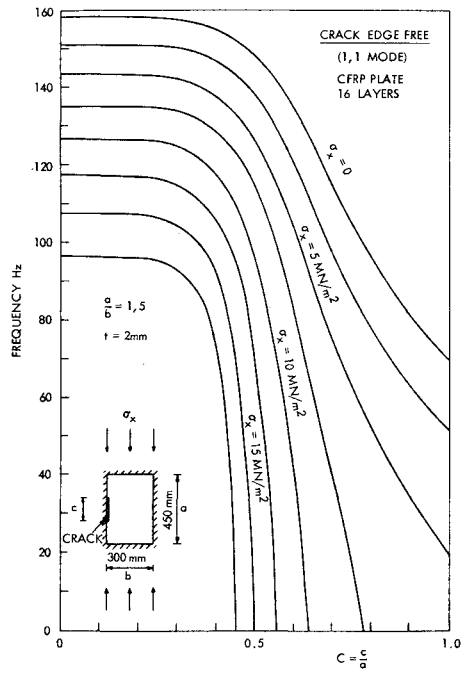


**Fig. 13 Effect of crack length and compressive stress on the natural frequency of the 1,1 mode of a CFRP plate.**

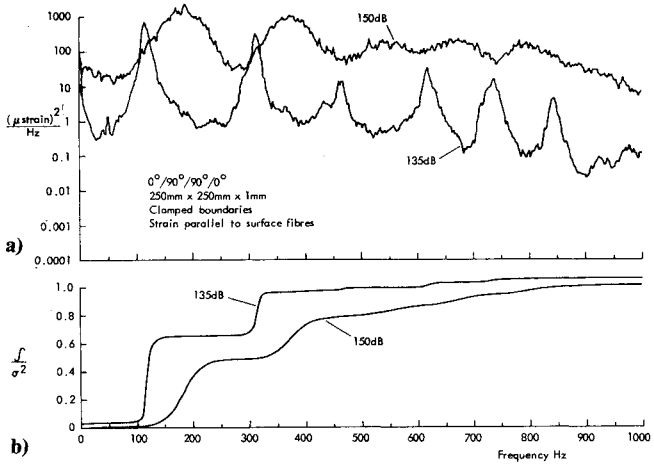


**Fig. 14 Strain spectral analysis for a thin CFRP plate; a) strain spectral density; b) (integral across strain spectral density)/mean square strain.**

was the case in the previous model, and various degrees of rotational constraint will be used at the boundaries.

## VI. Acoustically Induced Panel Vibration and Structural Response Prediction

In service, aircraft structures are subjected to dynamic loading which may cause fatigue damage. This is particularly a problem for panels that may be subjected to very high intensity acoustic excitation in regions close to engine effluxes. A considerable amount of research has been carried out in the past concerning the prediction of dynamic strains induced in aluminum alloy structures. A major part of that effort has been concerned with the development of simple methods for response prediction using fundamental mode approximations for estimating induced strain levels under the action of random, acoustic excitation.[9] Such methods rely on the assumption of linear behavior and use the normal mode approach, both having been quite well validated for aluminum alloy structures. However, the use of new structural materials, such as carbon fiber reinforced plastics necessitates some reappraisal of the "engineering" approach to dynamic response prediction.

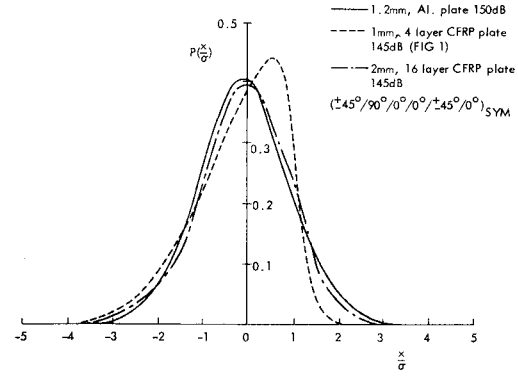


**Fig. 15 Normalized probability density of acoustically induced strains.**

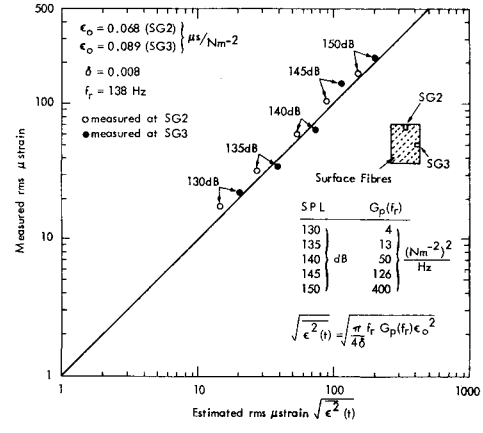


**Fig. 16 Comparison of measured and estimated rms strains in the 16-layer CFRP plate.**

A series of experiments carried out to examine the spectral and statistical properties of acoustically induced strains in thin aluminum alloy and CFRP plates has been reported upon in Ref. 10. The apparatus used for excitation consisted of a large horn, exponential in shape about one axis and tapered along the other, with a rectangular cross section. The 7 m × 3m horn was driven by an electropneumatic exciter and had a sound absorbing termination at the other end. The test section had the facility for mounting test panels, clamped in steel frames, in the wall of the horn so that they were clamped on all four boundaries and excited at grazing incidence. The panels were excited at grazing incidence. The panels were excited at overall sound pressure levels between 130 and 150 dB over a frequency bandwidth from 80 to 800 Hz using random excitation. The dynamic strain response of a 250 × 250 × 1.2 mm aluminum alloy panel was found to be essentially linear in nature and statistical analyses of the strain signals further validated the use of the simple Gaussian distribution for response description under random excitation. Strain spectral characteristics of the thin. (1 mm) four-layered CFRP plate are indicated in Fig. 14. The highly nonlinear nature of the response at high levels of acoustic excitation is clear in Fig. 14a, as shown by the broadening and flattening of the resonance peaks in the spectral density at the higher excitation level. This type of nonlinear behavior was much greater for the CFRP panel than for the aluminum alloy panel of similar thickness. The integrals across the strain spectral densities in Ref. 10, of the form shown in Fig. 14b,

showed that at 135 dB excitation level modal contributions were clearly evident in the response. At higher levels a "rounding" effect occurred at each step in the integrated plot and it is clear from the two curves in Fig. 14b that in the case of the CFRP panel the mean square strain was very much governed by spectral components throughout the whole bandwidth excited. At high sound pressure levels, the overall nonresonant response of the CFRP panel formed a very significant contribution to the mean square strain; only 65% of the mean square strain was due to resonance peaks compared with 90% for the aluminum alloy structure.

Probability density functions of acoustically induced strains in some plates are given in Fig. 15. The plots for the 1.2-mm-thick aluminum alloy plate and the 2 mm 16-layer CFRP plate are very similar in shape to a Gaussian distribution. That for the thin, four-layered CFRP plate indicates the lack of suitability of the Gaussian distribution for life prediction when nonlinear effects are present in the response; skewness values of up to 1 and kurtosis values in the range 2.6-5 were measured. The thin aluminum alloy and thick CFRP panel yielded probability distributions which were very symmetrical with skewness close to zero and kurtosis values close to three, justifying representation by the Gaussian distribution. Studies of nonlinear behavior of homogeneous beams, which have been carried out recently, have shown that reliable theoretical models for dynamic response and fatigue life predictions can be made at large vibration amplitudes under the action of random loading.[11,12] The predicted and measured strain probability distributions were in quite good agreement and showed evidence of characteristics similar to those observed and presented here for plates. It is apparent in experimental studies on thin composite plates, however, that other mechanisms might also cause nonlinear behavior in addition to large amplitude effects. It is also noteworthy that reasonable predictions of peak strain distributions were also obtained in Ref. 11 using relatively simple theoretical models, but further work is needed on the nonlinear forced vibration of anisotropic plates.

It is clear from Fig. 15 that prediction of rms strains in thin CFRP plates composed of a few layers is not possible using simple, modal theory when the structure is subjected to high-intensity acoustic excitation. It is clear, however, that thicker multilayered plates exhibit essentially linear behavior at fairly high excitation levels. It was found, for example, that the mean square strains in the 16-layer (2 mm) plate were predominantly (70-90% depending on measurement position) due to response in the fundamental mode. The single-mode approximation method for response prediction was therefore studied for this CFRP structure; this is the method[9] which has been successfully applied by Clarkson to metallic structures. The mean square strain in the panel is given by

$$\epsilon^2(t) = (\pi/4\delta) f_r G_p(f_r) \epsilon_0^2$$

where $f_r$ is the resonance frequency (Hz); $G_p(f_r)$ the spectral density of the sound pressure at $f_r$ ( $|\mathrm{Nm}^{-2}|^2$/Hz); $\delta$ the viscous damping ratio; and $\epsilon_0$ the strain at point of interest due to a uniform static load of unit magnitude (strain/$\mathrm{Nm}^{-2}$).

The pressure spectral density was measured via digital analysis of signals from microphones mounted in the acoustic test facility. Damping was measured via decay tests. The value of $\epsilon_0$ was derived via tests carried out on a static pressure loading rig which enables $\epsilon$ to be measured as a function of static pressure, the slope of the plot yielding $\epsilon_0$. The estimated strains were then derived via the above equation and are compared with measured strains in Fig. 16. Good agreement is evident in the figure and predicted strains were generally lower than measured strains because the fundamental mode approximation neglects response contributions in higher modes.

## VII. Conclusions

The approximate, fundamental mode approach which has been used successfully in the past for the prediction of random acoustically induced strains in metallic structures may be used for thick multilayered CRFP plates and Gaussian statistical properties may be used for response description. Thin structures of few layers, however, exhibit gross nonlinear behavior which precludes the use of such methods.

The free-vibration characteristics of homogeneous and composite plates with static in-plane compression may be predicted accurately via conventional theoretical methods incorporating measured material properties. Techniques have been established for measuring both the elastic and loss components of dynamic flexural and shear properties under simple and combined loading conditions.

It has been shown that the stiffness and damping properties of composites may be influenced by choice of fiber aspect ratio and a compromise between stiffness and damping characteristics may be achieved. However, to achieve significantly increased loss factors, the matrix material (resin) has to be chosen carefully.

## References

[1] Wright, G.C., "Dynamic Behaviour of Fibre Reinforced Plastic Beams and Plates," Ph.D. Thesis, Southampton Universtiy, Southampton, England, 1974.

[2] Abdin, E.M.Y., "Dynamic Properties of Some Carbon Fibre Reinforced Plastics," Ph.D. Thesis, Southampton University, Southampton, England, 1983.

[3] White, R.G., "Some Measurements of the Dynamic Properties of Mixed Carbon Fibre Reinforced Plastic Beams and Plates," *Journal of the Royal Aeronautical Society*, Vol. 79, No. 775, 1975, p. 318.

[4] Hooker, R.J., "High Damping Metals," Ph.D. Thesis, Southampton University, Southampton, England, 1975.

[5] Cox, H.L., "The Elasticity and Strength of Paper and Other Fibrous Materials," *British Journal of Applied Physics*, Vol. 3, March 1952, pp. 72-79.

[6] McLean, D. and Read, B.E., "Storage and Loss Moduli in Discontinuous Composites," *Journal of Material Science*, Vol. 10, 1975, p. 48.

[7] Teh, C.E. and White, R.G., "Dynamic Behaviour of Isotropic Plates under Combined Acoustic Excitation and Static, In-Plane Compression," *Journal of Sound and Vibration*, Vol. 75, No. 4, 1981, pp. 527-547.

[8] Teh, C.E., "Dynamic Behaviour and Acoustic Fatigue of Isotropic and Anisotropic Panels Under Combined Acoustic Excitation and Static, In-Plane Loading," Ph.D. Thesis, University of Southampton, Southampton, England, 1981.

[9] Clarkson, B.L., "Stresses in Skin Panels Subjected to Random Acoustic Loading," *The Aeronautical Journal of the Royal Society*, Vol. 72, 1968, No. 695, pp. 1000-1015.

[10] White, R.G., "A Comparison of Some Statistical Properties of the Response of Aluminium Alloy and CFRP Plates to Acoustic Excitation," *Composites*, Vol. 9, Oct. 1978, pp. 251-258.

[11] Bennouna, M.M. and White, R.G., "The Effects of Large Vibration Amplitudes on the Dynamic Strain Response of a Clamped-Clamped Beam with Consideration of Fatigue Life," To be published in the *Journal of Sound and Vibration*, Vol. 95, No. 2, 1984.

[12] Bennouna, M.M. and White, R.G., "The Effects of Large Vibration Amplitudes on the Fundamental Mode Shape of a Clamped-Clamped Uniform Beam," *Journal of Sound and Vibration*, Vol. 95, No. 2, 1984.